Bachelor Thesis

Nanosprings and the Electric Double Layer

Author: Janice van Dam

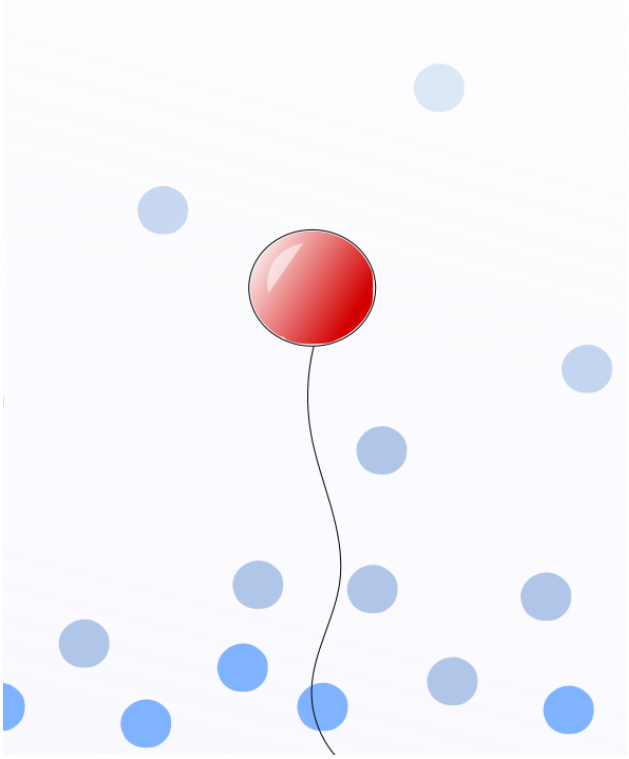

Supervisors: Dr. ir. Sanli Faez
Zhu Zhang Msc.

Utrecht University
Faculty of science
Department of physics
June 2020

Writing period

05. 02. 2020 – 19. 06. 2020

Supervisors

Dr. ir. Sanli Faez

Zhu Zhang Msc.

Abstract

The electric double layer (EDL) is a very important aspect in surface science. Small objects on the surface around which the EDL has formed can change the composition of the EDL. This change can be used to detect small objects. We have prepared a setup in which we can use this technique to visualise a nanosping, which then can be used to determine the mobility of a particle. The setup consisted of a potentiodynamic optical contrast microscope and conductive sampleslides. The samples we created are PEG linkers adhered to an ITO surface, to act as the nanosprings, with gold nanoparticles on top.

To give advice on specific parameters to use in the experiments, we created a simulation in python. In the simulation, a nanoparticle is subject to spring, drag and electric forces as well as Brownian motion. In the electric field, some influences of the electric double layer were introduced in the form of the so-called Debye Hückel approximation.

Upon analysing the simulation data my advise on carrying out the experiment as described in part I is to use a timestep between $dt = 10^{-5}$ and $dt = 10^{-3}$ s. For the simulation, my advice would be to use $N_t = 10^5$. For optimal results, the length nanospring should around 25 nm, with an applied potential of around 0.07 V.

Contents

1. Introduction

When an object is exposed to a material with mobile ions, a structure of charges, know as the electric double layer (EDL), forms around the object [1]. This EDL has been a popular topic of research since Herman von Helmhotz first realized its existence in 1853 [2], after which a lot of theory has been developed around this concept.

As small objects such as proteins are placed on a surface surrounded by an EDL, the composition of the double layer is altered slightly. This alteration gives rise to an important aspect of EDL research, as these changes in the EDL can be used to detect or visualise nano-objects on the surface. A good example of this method is a study on protein imaging done by Sotres and Baró [3]. They used an atomic force microscope to detect the forces between charged surfaces due to the electric double layer. A different illustration of its application is given by Li et al. in 2007 and Hamou et al. in 2009, where they probed the electric double layer using scanning electrochemical potential microscopy [4, 5]. These methods, however, do not operate on a single protein level.

A method for identification of proteins on a single protein level has been addressed by Ma et al. in 2018 [6]. In their experimental study they oscillate proteins in an alternating electric field. The proteins are linked to an conducting sampleslide. They use a near field imaging method to determine the charge, size and mobility of the proteins. Ma et al. used a few simplifications in their theory which are not necessarily justified. Where they assume scattering contrast is equivalent to particle size, intensity in the oscillation is equivalent to particle displacement and some applied potentials are too large for their formulation of the equation of motion, they leave some room for improvement. This method of using an oscillating spring to determine properties of the particle could also be used without taking into account the EDL, but that would only be valid in a non-aqueous medium. Taking into account the effects of the EDL thus makes this a more useful tool in biological measurements, where there is often an aqueous medium present.

Namink in 2019 [7] worked on a custom microscope utilized by the nanophoronics

group of Utrecht University. The microscope is a potentiodynamic optical contrast microscope, which also uses the EDL to detect the optical polarizability of particles. Computer simulations of the EDL are an important part in developing the theory and understanding its limitations. They can form the bridge between theory and experiment by predicting outcomes under certain circumstances. There are numerous simulations available on the dynamics of the EDL. In 1990 a Monte Carlo simulation was developed of the EDL by Svensson et al. [8]. Many authors have also reported on molecular dynamics calculations [9, 10, 11].

Combining the techniques of Ma et al. and Namink, we created an experimental setup. We designed this setup to test the application of the potentiodynamic optical contrast microscope on biomolecules and to measure the contrast of anchord nanoparticles. In addition, this setup could be used to study the electrophoretic mobility of gold nanoparticles connected to a surface via a polyethylene glycol linker.

Later in the project the focus shifted to simulating. The goal of the model is to capture the electrophoretic mobility of a nanoparticle connected to a nanospring, in the presence of an electric field which is influenced by the EDL. While simulations of spring-mass systems are very standard and the EDL has also been modeled numerous times, the combination of the two, which is very specific for the experimental setup, I have yet to find.

With the data of this simulation, we can predict the outcomes of the experimental setup. These predictions can be used in experiments to provide the right input for experiments and to verify results. The input can be the runtime needed for a certain accuracy of calculating the spring constant or the mobility of a nanoparticle or the optimum values for the spring length and applied potential.

2. Background and theory

In order to make a simulation of a nanospring, we need some theory to understand the physics. In this chapter I will first go through some general concepts that are important to understand the physics of the setup. I will explain some theory of the electric double layer, electrophoresis and Brownian motion. Then, I will derive the equation of motion that is used to simulate the behavior of the particle on the spring. I will also briefly touch the subject of floating point errors.

2.1. Electric Double Layer (EDL)

Many surfaces in an electrolyte solution develop a surface charge. These charges lead to a concentration gradient in the electrolyte which is referred to as the electric double layer.
The first explanation of the EDL was introduced by Hermann von Helmholtz, he saw that charged surfaces in solutions attracted counterions and repelled co-ions. In addition to this, Louis Georges Gouy and David Leonard Chapman observed that the electric potential from the counterions decayed exponentially away from the charged surface, introducing the *diffuse layer*. However, in the case of high surface charge, the Gouy-Chapmann model fails. Otto Stern combined to models of Helmholtz and Gouy-Chapman, which introduced the *Stern layer*. In this model, an electric double layer consists of the Stern layer and the (Gouy) diffuse layer, as can be seen in figure 1. The Stern layer consists of adsorbed ions, mainly due to non-electrostatic forces. The diffuse layer then is formed due to coulomb interactions, where it effectively shields the Stern layer from the bulk liquid. Together, the surface charge, Stern layer and the diffuse layer as the whole EDL is electroneutral.
The characteristic length scale of the EDL is the *Debye length*, given by

$$\lambda_D = \sqrt{\frac{\epsilon_0 \epsilon_r k_\mathrm{B} T}{2e^2 I N_A}}, \tag{1}$$

where ϵ_0 is the permittivity of free space, ϵ_r is the dielectric constant of electrolyte, k_B is the Boltzmann constant. The elementary charge is given by e, the ionic strength

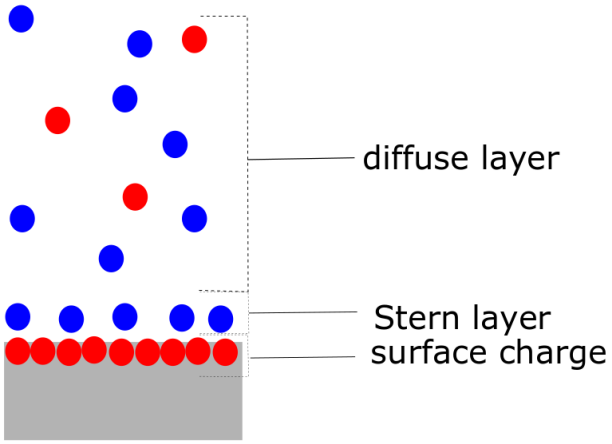

Figure 1.: Schematic representation of the electric double layer, including the surface charge, Stern layer and (Gouy) diffuse layer.

of the charged layers is given by I, and N_A represents Avogadro's number [12]. Along with the Debye length, another important length scale for the EDL is the *slipping plane*, which is the separation between the Stern and diffuse layer. Below the slipping plane, the charges are fixed, outside the plane charge can experience tangential motion relative to the charged surface. The electric potential on this plane is called the *Zeta potential* [13].

2.2. Electrophoresis

Electrophoresis describes the motion of charged particles in a fluid under a uniform electric field. The *electrophoretic mobility* is defined by $\mu_e = \mathbf{v}/\mathbf{E}$. The forces that play a role in this phenomenon are [13]

1. **the driving electrostatic force**, which is the coulomb force of the electric field acting on the surface charge;
2. **the frictional force**, the resistance due to the viscousity of the fluid;
3. **the electrophoretic retardation force**, this force is caused by the moving countercharge from the EDL. It depends on the composition of the EDL and the ionic mobility;
4. **the relaxation force**, this is by reason of non-coinciding charge-centers. A small dipole moment may be induced due to a shift in the EDL.

The latter force is neglected in the following approximated theories. Considering two cases: one in the limit of very thin EDL, and one in the limit of thick EDL.
The first limit gives rise to the Helmholts-Smoluchowski law [14], where the *electrophoretic mobility* is given by

$$\mu_e = \frac{\epsilon_r \epsilon_0 \zeta}{\eta}. \tag{2}$$

Here, ζ is the zeta potential as described in section 2.1 and η is the dynamic viscosity of the dispersion medium.
For the limit of a thick EDL, there is the Hückel-Onsager law [15]

$$\mu_e = \frac{2\epsilon_r \epsilon_0 \zeta}{3\eta}. \tag{3}$$

2.3. Brownian motion

Brownian motion is a noise first discovered by Robert Brown. It is a random movement of small particles. In the case of the simulation of the nanospring, we want to know the position of the particle on the spring over time. In this signal, there will be some noise due to the Brownian motion of the particle. This noise is especially vital in small signals, where the signal to noise ratio becomes very high. In describing a nanospring, we do expect the signal to be small enough for the Brownian motion to play a considerable role.
Brownian motion is traditionally described by a probabilistic process of the particles colliding with the fluid molecules, where the Brownian particles satisfy the diffusion equation,

$$\frac{\partial n(x,t)}{\partial t} = D \frac{\partial^2 n(x,t)}{\partial x^2}. \tag{4}$$

Here, $n(x,t)dx$ defines the number of particles at a position between x and $x + dx$ at a time t. And D is called the diffusion coefficient.
The motion can also be described by continuous Markov process theory, as suggested by Daniel T. Gillespie [16]. Gillespie describes a algorithm for an Ornstein-Uhlenbeck process, which is a category of Markov processes. It is also described how this Ornstein-Uhlenbeck process can be used to simulate Brownian motion when using the correct parameters.
For an overdamped system, Brownian motion is described by the Fokker-Plank equation [17]. For a system with drift $\mu(X_t, t)$ and diffusion coefficient $D(X_t, t)$, the Fokker–Planck equation for the probability density $p(x,t)$ of the random variable X_t

is [18]

$$\frac{\partial p(x,t)}{\partial t} = \frac{\partial}{\partial x}(\mu(x,t)p(x,t)) + \frac{\partial^2}{\partial x^2}(D(x,t)p(x,t)). \tag{5}$$

2.4. Equation of motion

The motion of a particle with radius a and mass m, in a medium with viscosity η in a general potential $U(y)$ can be described the equation of motion (following from Langevin's equation [19])

$$m\ddot{y} = -6\pi\eta a\dot{y} - \frac{dU}{dy} + X.$$

Where X is the random force resulting in thermal fluctuations. When in the overdamped regime, this equation simplifies to the case where $m\ddot{y} = 0$. This leads to

$$\dot{y} = -\frac{\frac{dU}{dy}}{6\pi\eta a} + \Gamma. \tag{6}$$

Where I have introduced the stochastic increment $\Gamma = \frac{X}{6\pi\eta a}$. The combination $6\pi\eta a$ is known as the Stoke's drag term. We require the long-time asymptote to be $\langle y^2 \rangle = 2Dt$, where $D = \frac{k_B T}{6\pi\eta a}$ is the diffusion coefficient [20] which also includes the Boltzmann constant k_B and the temperature T.
In the setup of this simulation, there are 3 main components to this equation:

1. The noise term, X;
2. the first term in the potential energy, resulting from the spring;
3. a second term in the potential energy, resulting from the applied potential and electric double layer.

Together, the 3 forces that govern the force balance of the particle are covered: the drag force, already present in equation (6) and the electric force and the spring force, both present in the $\frac{dU}{dy}$ term.
In the setup of the simulation, we are in the overdamped regime, where $\sqrt{\frac{k}{m}} < \frac{6\pi\eta a}{2m}$ [17], which justifies the use of equation (6). To understand what to write for the stochastic part, $\frac{X(t)}{6\pi\eta a}$, in the overdamped regime, we need a few ingredients. It is known that overdamped Bronwian motion is described by the Fokker-Plank equation [21]. We also have our restriction on the mean squared displacement, $\langle y^2 \rangle = 2Dt$. The amplitude is expected to be proportional to D, as it is without the overdamped

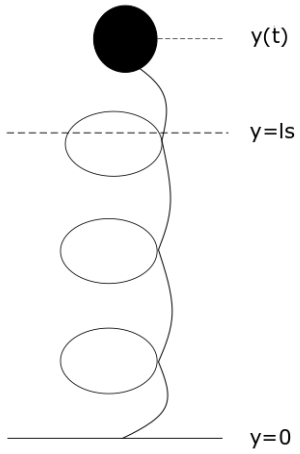

Figure 2.: Schematic representation of a particle on a spring. ls is the length of the spring in it's equilibrium position.

limit. This can be determined by examining the case with $U = 0$. From this, one can find that the mean squared displacement is equal to the mean square of the stochastic increment. We thus have the restriction $\langle \Gamma^2 \rangle = 2Ddt$. Now, to satisfy the appropriate Fokker-Planck equation we need to assume Gaussiality. From these things we conclude that the stochastic increment needs to be drawn form the probability distribution

$$P(\Gamma) = \frac{\exp(-\Gamma^2/4Ddt)}{\sqrt{4\pi Ddt}}. \tag{7}$$

The noise is thus drawn from a normal distribution with mean 0 and variance $2Ddt$, where dt is the timestep of the simulation. A more detailed derivation of this can be found in [20]

In the first term of the potential energy, the focus was on a particle on a spring with spring constant k. In this situation, the potential is given by $U(y) = \frac{kx^2}{2}$. Here, $x = y - l_s$ with l_s the length of the spring in equilibrium as in figure 2. Satisfying the long-time asympote is equivalent to being in line with the equipartition theorem $\langle E \rangle = k_B T$, or $\langle \frac{kx^2}{2} \rangle = \frac{k_B T}{2}$.

The next term in the potential energy is about the electric field. Besides the applied potential, which will be alternating, $V = V_0 \sin(\omega t)$ with ω the angular frequency, we also want to take into account effects of the EDL. A Debye Hückel approximation was used in the Gouy-Chapmann model of the EDL.

Combining Boltzmann statistics, the charge density of the ions and Poisson's equation

one can arrive at the Poisson-Boltzmann equation:

$$\frac{d^2\phi_\Delta}{dy^2} = -\frac{1}{\epsilon_r\epsilon_0}\sum_i n_i^0 z_i \exp\left(-\frac{z_i F\phi_\Delta(y)}{RT}\right). \tag{8}$$

Where n^0 is the particle density of species i with charge number z. F is the Faraday constant and R is the gas constant ($R = N_A k_B$). ϕ_Δ is identified as the potential energy.

Now we can make the Debye-Hückel approximation, which assumes that the potential variation is small,

$$\frac{zF\phi_\Delta(y)}{RT} << 1. \tag{9}$$

We then arrive at the expression for the potential

$$\phi_\Delta(y) = \frac{\sigma^M}{\epsilon_r\epsilon_0\kappa}\exp(-\kappa y) \tag{10}$$

where the charge density is given by

$$\sigma^M = \sqrt{8RT\epsilon_r\epsilon_0 c^0}\sinh\left(\frac{zF\phi_{\Delta,0}}{2RT}\right) \tag{11}$$

with κ the inverse Debye length given by

$$\kappa = \sqrt{\frac{2(zF)^2 c^0}{\epsilon_r\epsilon_0 RT}} \tag{12}$$

$\phi_{\Delta,0}$ is the applied potential, which is set to be

$$\phi_{\Delta,0} = V_0\sin(\omega t). \tag{13}$$

Now, to get an expression for the electric field (E) to plug into the equation of motion,

$$\dot{y} = -\left(\frac{k(y(t) - l_s)}{6\pi\eta a} - \mu E\right) + \Gamma, \tag{14}$$

we have to differentiate equation (10) with respect to y ($\frac{d\phi_\Delta(y,t)}{dy} = -E$), with equations (11) and (13) plugged in. The electric field is then given by

$$E = \sqrt{\frac{8RTc^0}{\epsilon_r\epsilon_0}}\exp(-\kappa y)\sinh\left(\frac{zFV_0\sin(\omega t)}{2RT}\right). \tag{15}$$

Which completes our expression for the equation of motion.

2.5. Floating point errors and dimensions

When working with large and/or small numbers in simulations one can have issues with floating point errors. These errors occur because of the finite number of digits a computer can store. In order to reduce the impact of these errors, the characteristic values in the equation of motion are preferred to be close to 1. This can be done by introducing dimensionless units. Dimensionless units are created using scaling factors, depending on each basic unit: time, mass, distance, temperature, electric current, luminous intensity and amount of substance.

Part I.

Experiment

3. Methodology and setup

In this section I will describe how to prepare the samples for two experiments. I will also describe some basic steps on operating the potentiodynamic optical contrast microscope.
The first is the landing check experiment, this is more of test experiment. This experiment can be used to get used to the setup and working with the microscope.
The second experiment is about nanosprings, which has the same setup as the simulation in part II. This experiment has the goal to study the electrophoretic motion of the nanoparticles that are attached to the nanosprings.

3.1. Landing check

To get used to the setup of the microscope, one can perform a landing check. Here, the goal is to be able to recognize nanopartiles landing on the glass surface of the sample slide. For this, the sample is to be prepared in 3 main steps: cleaning; preparing the flowcell; adding the particle solution. The protocol for the sample preparation is as follows.

1. Clean a glass slide of 24 by 40 mm (thickness #1) and a smaller 24 by 24 mm one, by rinsing with ethanol, isopropanol and DI water 2-3 times;

2. add the small glass plate on top using double sided tape, folded in half, to create the flow cell;

3. add a 10 times diluted poly-l-lysane solution to the flowcell, let sit for about 5 minutes, then rinse with DI water. This can be done by pipetting about 20-40 μL on one side of the flow cell and 'pulling' the liquid through by holding a piece of tissue on the other side (the solution will spread due to the capillary forces). This will provide a positive charge on the glass surface, so that the negatively charged particle can land on it;

4. add a 10 times diluted 30 nm gold nanoparticle solution.

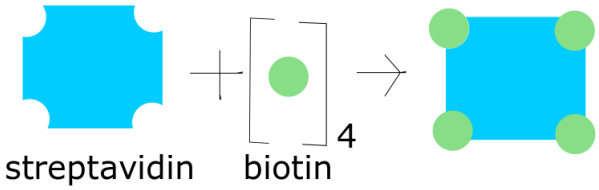

Figure 3.: Schematic overview of streptavidin-biotin binding.

3.2. Gold nanoparticle springs

We want to study the electrophoretic mobility of a particle on a spring, subject to an electric field. For this, we need to create nano-sized springs, with nanoparticles attached. To make sure we can apply an electric field, we used coverslides covered in an indium tin oxide (ITO) layer for conductivity.

To act as the springs, we used Polyethylene glycol (PEG) molecules. PEG molecules are of the form $H-(O-CH_2-CH_2)_n-OH$. On top of these PEG springs we adhered gold nanospheres by means of the straptavidin-biotin interaction. We used PEG springs that were functionalised with a biotin head and gold nanoparticles that were covered in straptavidin. Streptavidin is a protein with a very high affinity for the vitamin biotin. This high affinity is due to a combination of their shape complementarity, a network of hydrogen bonds and the hydrophobicity of the biotin binding pocket resulting in Van der Waal's interactions [22]. A schematic representation of the biotin bonding to the streptavidin protein can be found in figure 3.

We could then adhere the springs to the coverslips, in order to achieve this, we used PEG molecules with a silane group at it's tail. Silane is an inorganic compound, SiH_4. Silane molecules can form a hydrogen bond with a glass surface. Upon heating, this hydrogen bond can be made into a covalent bond as is schematically shown in figure 4.

Besides the biotin-PEG-silane molecules, we also used PEG-silane molecules without this funtionalisation. The PEG molecules without the biotin (mPEG) head act both as a surface passivation, to prevent non-specific binding [23], as well as spacers for the biotin-PEG's. Together, the samples should have a setup similar to that depicted in figure 5 with a roughly 1000:5 ratio of mPEG to biotin-PEG.

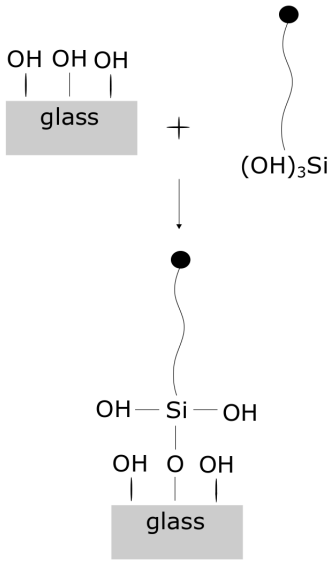

Figure 4.: The binding of silane to glass. The OH of the silane group at the tail of a PEG linker can form a bond with one of the OH's on the surface of a glass plate.

Materials

The materials we used for the preparation of these samples are

- 24 by 40 mm ITO plate, thickness #1;
- plasma cleaner + holder for the plates;
- mPEG-Silane-5000 (Laysan Bio item# MPEG-SIL-5000-1g);
- Biotin-PEG-Silane-5000 (Laysan Bio item# Biotin-PEG-SIL-5K-1g);
- etanol;
- acetic acid;
- DI water;
- streptavidin coverd gold nanoparticles.

Protocol

The preparation of the samples (partially based on 'PEG Coated Slides' protocol by Dogic Lab [24]) can be done in the following way

1. Clean the ITO plates using a plasma cleaner (to check, a slide is very clean when a drop of water has a very small contact angle, i.e. it spreads out very quickly and widely, see figure 6a);

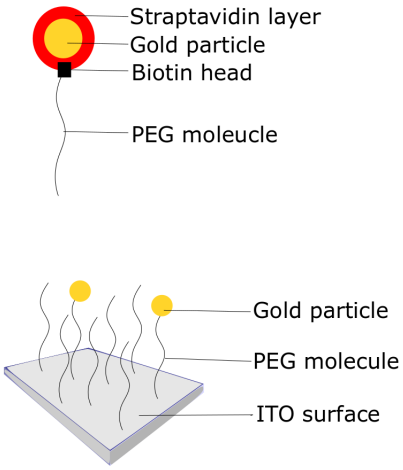

Figure 5.: Schematic picture of the sample slide. Two different kinds of PEG molecules are adhered to an ITO surface through a silane group on their tail. Some of the PEG molecules have a biotin head to which a streptavidin covered gold nanoparticle can adhere.

2. weigh out between 0.25 to 1 mg of biotin-PEG and 1-2 mg of mPEG using a microbalance;

3. make a ethanol + 1% acetic acid solution;

4. mix the ethanol solution and PEG's to create at least 50 μL of 0.5% PEG (with a 1000:5 mPEG to biotin-PEG ratio) in ethanol with 1% acetic acid;

5. sandwich 50 μL of the solution in between two ITO slides and let the liquid coat the two surfaces. Some liquid may spill out, but it is fine as long as both sides have an even coating, this method of distributing the liquid helps prevent micro beads from sticking to the surface;

6. incubate at 70°C for approximately 30 minutes, this allows the hydrogen bond between the silane group in the PEG and the glass surface to form into a covalent bond. Since the incubator might take a while to get up to this heat, make sure to set it to preheat before preparing the samples;

7. rinse with DI water to remove non-adhered PEG's (to check, a water drop should have a high contact angle, i.e. the drop should hold a drop shape on a

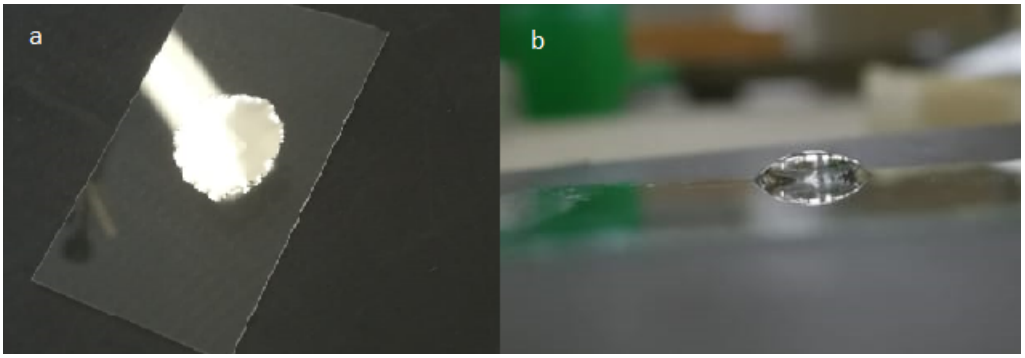

Figure 6.: Contact angle of a drop of DI water on a) a clean ITO surface (low contact angle, thus spread out) and b) a PEG coated surface (higher contact angle, thus retaining their 'drop' shape).

PEG gelated surface, see figure 6b)

8. add the streptavidin covered gold nanoparticles;

9. make a flow cell with this ITO plate: place two pieces of double sided sticky tape, folded in half, on the ITO plate. Add a smaller, square ITO plate (doesn't need to be glass, or coated with the PEG layer) on top. This way, the height of the flow cell will be around 160 - 200 micron, depending on how firm the fold of the tape is.

3.3. Handeling the microscope

After preparing the samples from the previous sections, we can look at them with a microscope. We created the sample to be viewed with the potentiodynamic optical contrast microscope that is present in the nanophotonics group at Utrecht University. To understand how this microscope works I will give a brief explanation.
Potentiodynamic optical contrast microscopy is a form of dark field microscopy. In dark field, as the name suggests, the background of a picture (or the field of view) is dark, and the object is illuminated. It works by collecting scattered light, rather then the whole of the incident light beam that remains unscattered, as in light field microscopy. The object is then illuminated in the picture, because this is what scatters the light onto the objective.
Since the sampleslides are coverd in ITO, the surface potential can vary. A change in electrode potential then results in a change in the elastic light scattering from the sample. This change in elastic light scattering is referred to as *potentiodynamic*

optical contrast and it can be used to visualise the electric double layer. Movements of the particles on the spring will cause a change in the composition of the EDL, which can be visualised using this potentiodynamic optical contrast microscope. A more detailed description on the microscope can be found in the master thesis of Kevin Namink [7].
The first step of operating the microscope is to turn on the laser, since it takes about half an hour to warm up, do this before preparing the sample. When the sample is ready, you can place it on the objective. First clean the surface with iso-propanol before adding a new drop of immersion oil. Place the sample being careful not to spread the immersion oil too much. There are two tiny magnets to make it stay in place.
Once the laser, the camera and the computer are turned on, click 'startprogram' and select a nice region to look at by dragging the yellow lines. Then focus on dust speckles on the ITO surface using the manual focus knob. After that, the piezo focus loop can be started.
A piezoelectric actuator, or piezo for short, uses the piezoelectric effect to convert the electrical energy to mechanical displacement. When a piezo is connected to a proportional–integral–derivative (PID) controller it can be used to very accurately control and stabilize the position of a sample. A PID controller is a device that keeps a certain value stable. It calculates the error, which is the difference between the desired setpoint and a measured process variable, then applies corrections. The corrections have three terms:

1. **Proportional** This term gives corrections proportional to the current error;

2. **Integral** Is the sum of the instantaneous error over time, giving an indication of how far off the proportional term was in correcting;

3. **Derivative** Can be calculated by the slope of the error over time multiplied by the rate of change of the *gain*, which is how much the output is changed in response to a change in error.

To make the device work properly, the control loop has to be tuned in order to make signal, that is send to the piezo, stable, responsive and have minimal overshooting. We can not optimize all of these properties simultaneously, so we need to obtain a balance between them.
For the experiment with the ITO and PEG coatings, an electric field can be applied between the two plates of the flowcell.

To save any data: start and stop recording in the period you want to save, the file path can be changes on the left of the screen. Copy data onto external hard-drive to analyse it.

4. Results

4.1. Landing check

When doing the landing check experiment, one can see the particles landing by looking at the microscope screen. The particles will move around, come into focus and then stop, where they will stick to the surface, where the microscope is focused on. To analyse this further, the data was put in a python script written by Namink [7].
A landed particle will stay in one place, in all dimensions. Being stable in the z-direction can be seen by a constant value for the intensity. The script uses a background correction that sets the average of the 5 previous images as the background for the current one. This correction leads to a linear decay in intensity for the landed particles over 5 frames, after which they will disappear in the background. This decay can be seen in figure 7(a), which shows the relative intensity over time for each landed particle. The total intensity for each landed particle is plotted in figure 7(b). As a further improvement of the background corrections I implemented a subtraction of a snapshot of the camera with the laser turned off. On this snapshot one can see a few dots, which may influence the appeared intensity of a particle at certain spots. To check if the distribution in intensities had a connection with the background intensity I made a few plots.
From looking at the background I don't see many irregularities per frame. There is no specific region lighter or darker and so the intensity of the background seems rather uniform aside fromm a few small speckles. To check this, I made a plot that shows the intensity of a landed particle as their dot size at their landing position in figure 8(a). Here you can see that there is a clear difference in intensity for different landed particles, but not a clear pattern in space. It seems, however, that there is a difference in overall intensity per frame. Therefore, the difference in intensity for different particles might be explained by their different landing times. To see the influence of time, I plotted the total particle intensity as a function of their mean background intensity in figure 8(b). This is after subtracting the 'dark' background.

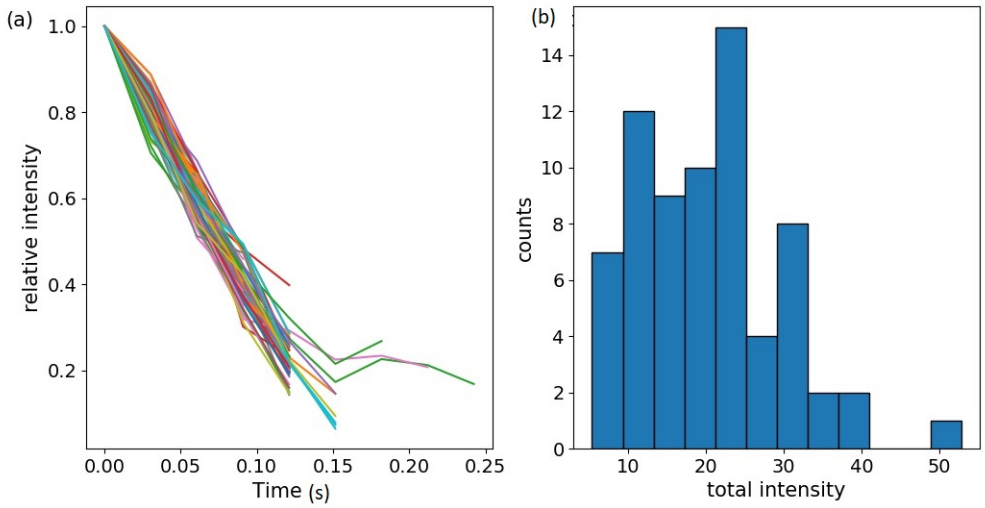

Figure 7.: (a) intensity change over time per landed particle (b) total intensity per landed particle.

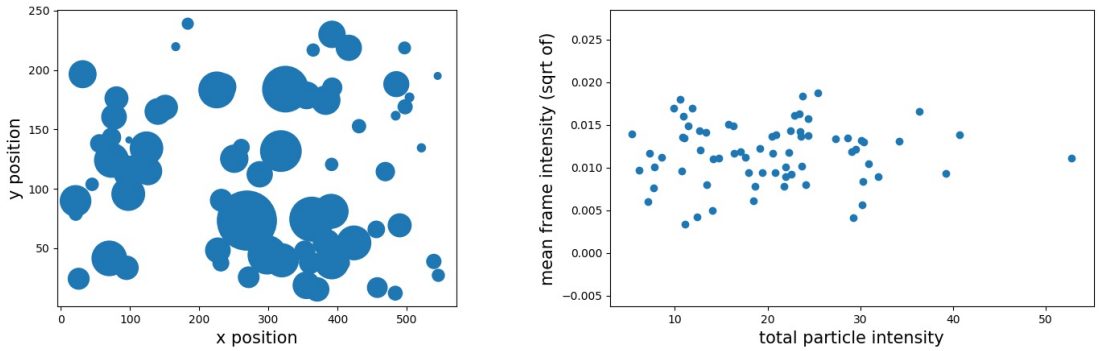

Figure 8.: Figures to determine the impact of background differences to the particle intensity in a) space: The intensity of each landed particle, indicated by the size of the dot, and their landing positions and b) time: Total intensity of a landed particle as a function of the average frame background intensity.

4.2. Gold nanoparticle springs

Unfortunately I was not able to get any usable data from this experiment as COVID-19 hindered my time in the lab.

Part II.

Simulation and analysis

5. Methodology

We want to be able to describe and predict possible outcomes of the experiments under certain circumstances, like the amount of datapoints and the timesteps between them, different spring lengths, and different applied potentials. This way, you would have to do less experiments in order to get the desired results. To make these predictions, we made a simulation in Python. The goal of the python script is to simulate a nanoparticle on a spring in an electric field, which is the setup of the experiment described in section 3.2. We can then look at the outcomes of the simulation in the analysing script.

5.1. Simulation

The most important part of this simulation is the equation of motion that describes the motion of the particle. This equation of motion is derived in section 2.4 and given by equation (14). To be able to use this equation of motion, we have to rewrite it as an update formula. We can discretize the equation of motion using Euler's method, to get

$$y(t+dt) = y(t) - \left(\frac{k(y(t) - l_s)}{6\pi\eta a} - \mu E \right) dt + \Gamma. \tag{16}$$

In a simple loop, the values for the electric field and the position can be calculated at each timestep and put into an array, ready to be saved or plotted.
For the initial value of the position, we take the length of the spring in equilibrium, l_s.

5.1.1. Values and Units

One of the most difficult things in simulating is making sure the numbers you plug in make sense, and are compatible. A way to check on these values is to keep them in a table, like the one included in the appendix. Some sanity checks include:

1. the variations in the positions (y) should be less, or at least not much bigger than the length of the spring in equilibrium, l_s;

2. when the E-field is set to zero, the position distribution should be a gaussion, and the mean squared displacement should satisfy the equipartition theorem;

3. the length of a PEG molecule can be calculated based on the PEO unit length of 0.28 nm in water [25], this article also gives an estimation on what to use for the spring constant of the PEG;

4. the noise term should not overshadow the rest of the equation of motion, as the particle will then just 'drift' away.

When considering the scaling factors to reduce the floating point errors as described in section 2.5, we consider the important terms in the equation of motion (14) The only scaling factors that we have to deal with in this equation of motion are those for time and distance, introduced in the simulation as T_0 and R_0 respectively. Other dimensions either don't occur or drop out.
The important quantities in this simulation are

1. $\frac{k}{6\pi\eta a}$, which has basic dimensions $\frac{1}{T_0}$;

2. dt, which has basic dimensions T_0;

3. μE, which has basic dimensions $\frac{R_0}{T_0}$;

4. D, which appears in the stochastic increment and has basic dimensions $\frac{R_0^2}{T_0}$.

Characteristic values in the simulation are nanoseconds for time and Debye lengths for distance, the values for R_0 and T_0 were thus set to be 10^{-8} and 10^{-9} respectively.

5.1.2. Time

Naively one could draw random values from a unit normal distribution do describe Brownian motion. The problem that arises is the time, where the timesteps of the noise have to align with the timesteps of the deterministic part of the equation of motion ($\frac{\frac{dU}{dx}}{6\pi\eta a}dt$). Therefore the normal distribution has it's particular width.
For a successful simulation, the timesteps and runtime need to be carefully considered. The typical forces, velocities or displacements in the system should have changes in each step that are 10-100 times smaller then the timestep in order to resolve the relevant physics.
As the magnitude of the stochastic increment goes like $\sqrt{dt}$ and the deterministic part goes like dt, a small dt results in the noise being dominant. You will need a long runtime in order to see effects of the deterministic part. Whereas with a large dt the

deterministic part is dominant.
In the simulation we deal with several damping times. The first damping time is that of the spring. This damping time assures us that we operate in the overdamped regime, as stated before. A different damping time that plays a role is that of the Brownian motion, $\tau_p = \frac{m}{6\pi\eta a}$ [17] which is around half a nanosecond in our system.
For the oscillation frequency of the electric field, we have to take into account the time it takes for the EDL to form, and thus for the whole system to react to the change in field. If the electric field oscillates too quickly, the system will not have time to adjust. This time is known as the charging time and is given by $\frac{a}{\kappa D} = 4.5 \cdot 10^{-6}$ ns [26], so with any frequency below $2.3 \cdot 10^4$ Hz it should be fine.

5.2. Analysing script

An analysing script was created to retrieve certain values from the simulation. With this, one can, for example, examine the amount of data points needed for a certain precision of extracting the zeta potential.
Because of the long term asymptote of the Brownian motion, we can easily extract the spring constant from a dataset with zero applied potential. We can use $\langle (y - ls)^2 \rangle = \frac{k_B T}{k}$ to determine k. In these types of calculations we have to be careful in which system of units we are working: the scaled units in nanoseconds and Debye lengths or SI units?
If we want to calculate the zeta potential, we need this calulation of the spring constant. We then also need a second dataset, with applied potential. To carry out this calculation we need to filter out the noise in the signal due to Brownian motion. This can be done by Fourier transforming the signal and applying a low pass filter on the frequency of the applied potential. This can be done by Python's scipy.fftpack. This pack includes a fast Fourier transform (FFT) and inverse FFT.
The filtering is done in 3 steps:

1. making an fast Fourier transform (FFT) of the signal using scipy.fftpack.fft;

2. applying the low pass filter by setting all frequencies above the applied frequency to zero;

3. getting the filtered signal back by applying inverse FFT to the peak using scipy.fftpack.ifft.

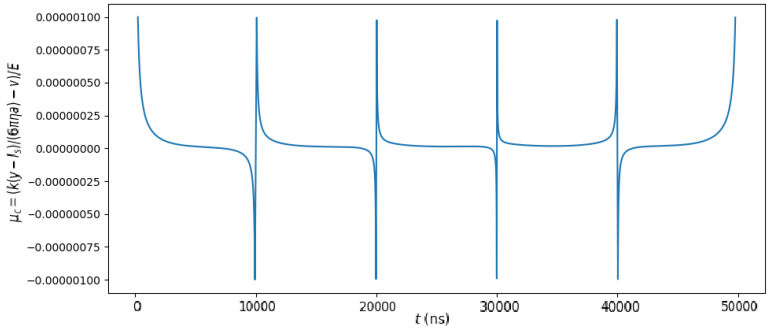

Figure 9.: Calculation of μ at each timestep, where the peaks come from the electric field passing 0.

We can now use the force balance $F_{\text{drag}} + F_{\text{spring}} + F_{\text{electric}} = 0$ to obtain

$$v = \frac{k(y - l_s)}{6\pi\eta a} - \mu E. \tag{17}$$

Where v can be found using numpy.gradient(y). From this, μ can be determined, and thus the zeta potential, $\zeta = \frac{\mu\eta}{\epsilon_r \epsilon_0}$.
The force balance equation should be satisfied at each point in time, but as the mobility goes like 1/E, it behaves strangely every time the electric field passes zero, so the mobility is not well defined at this point. This behaviour can be seen in figure 9. To overcome this, I apply a 'filter' and only use the points for which the absolute value of the electric field is more then 50% of its maximum. Figure 10 shows the components of equation (17).

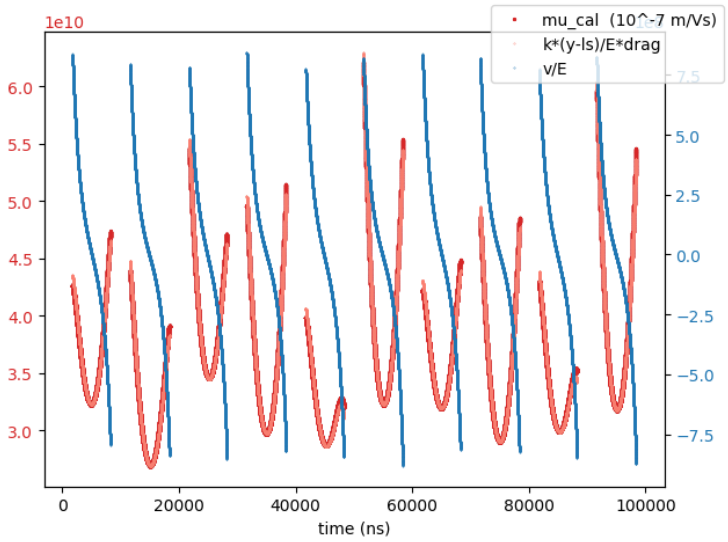

Figure 10.: Overlap plot of all components in the force balance equation (17) after filtering the electric field to be at least 50% of its maximum.

6. Results

We can get some different results from the data generated by the simulation. These results come from different datasets. The calculation of the spring constant, for example, does not include the electric field. The most general settings are given in the appendix, when some different parameters are used this will be indicated.

6.1. Equipartition

For a particle on a spring subject to Brownian motion, so when the E-field is set to 0, we expect it to satisfy the Equipartition theorem. Theoretically, this can be used to check the simulation on correctness. Experimentally this can be used to identify if particles are stuck to the surface or moving. When calculated at different timesteps, we can find which values for dt are appropriate for resolving the relevant physics in the simulation.
According to Bolzmann the position distribution should be a Gaussian [27], which was indeed the case as seen in figure 11.
To check the simulation's sensitivity to the equipartition theorem at different timesteps, we have figure 12. In this figure the fractional difference is shown for different dt, the amount of simulation points was set at 5 million.

6.2. Spring constant

With the electric field set to zero, we can retrieve the spring constant by analysing the Brownian motion and using the equipartition theorem. Using $k_{\text{calc}} = \frac{k_B T}{\langle (y - l_s)^2 \rangle}$ we calculated the spring constant. The input value for the spring constant in the simulation was $k_{\text{input}} = 6 \cdot 10^{-4}$ N/m. In figure 13 we calculated the spring constant for different amounts of datapoints (N_t), and I show their fractional difference with the input value for the spring constant. For which I used $dt = 10^{-5}$ seconds. For each N_t the calculation was repeated 100 times and the result was taken to be mean $\pm$ standard deviation.

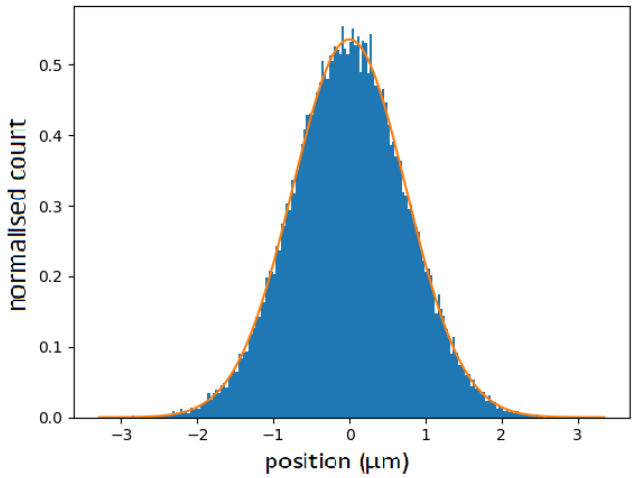

Figure 11.: Position distribution of a particle on a spring with the effect of Brownian motion (blue) with fitted gaussian (orange). With dt = 0.001 s, T = 50000.

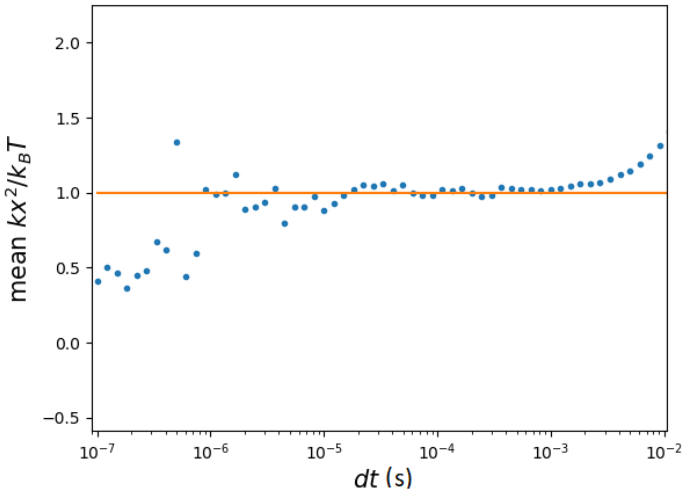

Figure 12.: Deviation from equipartiotion (at $k\langle x^2\rangle/k_{\mathrm{B}}T = 1$) at different orders of magnitude for the timesteps for a constant number of datapoints $N_t = 5 \cdot 10^6$.

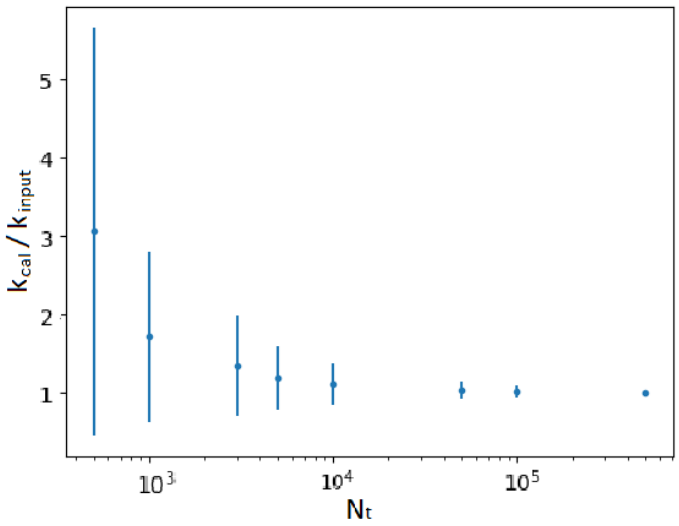

Figure 13.: The calculated spring constant, $k_{\text{calc}} = \frac{k_B}{\langle (y-l_s)^2 \rangle}$, for different numbers of datapoints, N_t. Shown divided by the input value of the spring constant of $k_{\text{input}} = 6 \cdot 10^{-4}$ N/m. The timestep used was $dt = 10^{-5}$s. The values and errors are the mean and standard deviation of the experiment repeated 100 times.

6.3. Filtering

The next step it to filter the second dataset, which includes the electric field. The result of this filtering can be found in figure 14

6.4. Mobility

If we calculate the mobility in the way described in section 5.2, we get a result as shown in figure 15. From the values in the plot we can calculate the mean and standard deviation of the calculated mobilities. We can then propagate the uncertainty of the calculation of the spring constant by means of the variance formula to find $\mu_{\text{calc}} = (3.43 \pm 0.24) \cdot 10^{-8}$ m^2/Vs. For reference, the input value was $\mu_{\text{input}} = 3.55 \cdot 10^{-8}$ m^2/Vs.

We can then repeat the same calculation multiple times, like we did in the calculation of the spring constant, and to the same for different values of the spring length. In figure 16a I show the fractional difference of the mobility with its input value for

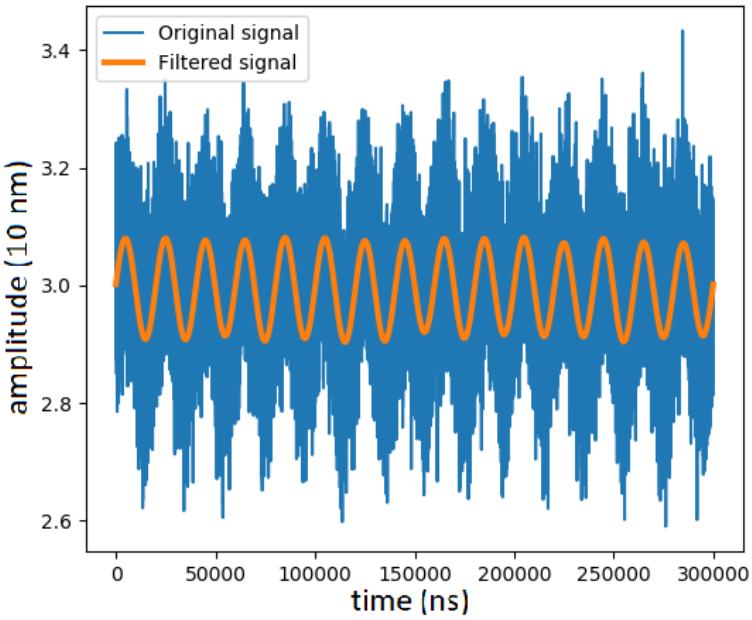

Figure 14.: The original signal, containing Brownian noise, and the signal after filtering using FFT.

different spring lengths. For any spring length less than 18 nm, the simulation was not able to handle the data as the electric field became too large. In 16b I show the spread of the first 50 repetitions of the calculation for a spring of 60 nm long.
After this, I generated data for different applied potentials V_0, using a spring length of 25 nm. In table 1 I show the values from these calculations.

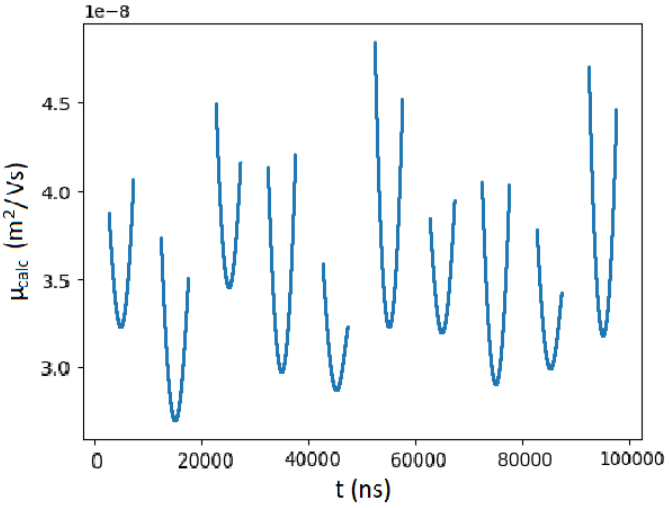

Figure 15.: μ calculated at the points in time for which the electric field is at least 50% of its maximum, using the force balance from equation (17). Shown relative to $\mu_{\text{input}} = 3.55 \cdot 10^{-8}$ m^2/Vs and calculated with $dt = 10^{-5}$ s and $N_t = 10^5$.

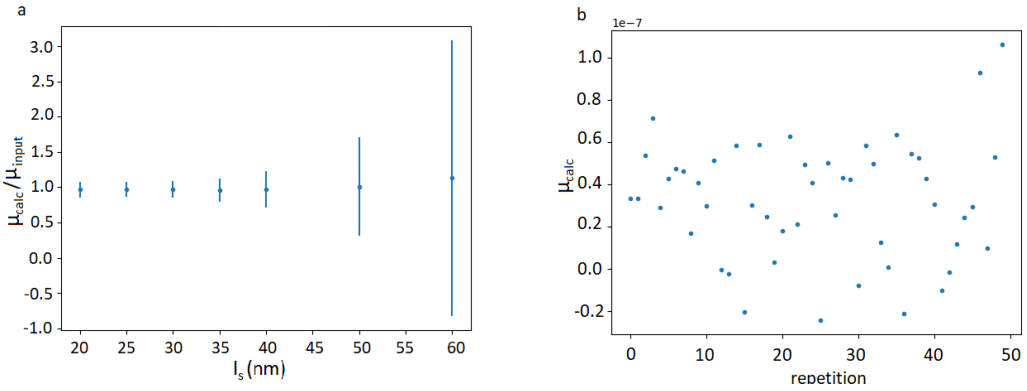

Figure 16.: μ calculated at the points in time for which the electric field is at least 50% of its maximum, using the force balance from equation (17). Calculated with $dt = 10^{-5}$ s and $N_t = 10^5$. a) Shown relative to $\mu_{\text{input}} = 3.55 \cdot 10^{-8}$ m^2/Vs. The values and errors are the mean and standard deviation of the experiment repeated 100 times for different spring lengths l_s. b) Shown for the first 50 repetitions of the calculation for $l_s = 60$ nm.

V_0 **(V)**	μ_{calc} **(m^2/Vs)**	σ_μ
0.001	8.78E-08	3.23E-07
0.005	3.47E-08	6.62E-08
0.01	3.59E-08	3.16E-08
0.05	3.50E-08	5.48E-09
0.07	3.55E-08	3.99E-09
0.1	3.43E-08	4.03E-09
0.2	NAN	NAN

Table 1.: Calculated mobility, μ_{calc}, after 100 repetitions and its standard deviation, σ_μ for different values of the applied potential, V_0. Calculated with $dt = 10^{-5}$ s, $N_t = 10^5$ and $l_s = 25$ nm.

7. Discussion and conclusion

Here, I will discuss the results shown in the previous section. With this, I will also draw conclusions about experimental settings and give experimental advise.

7.1. Equipartition

For the simulation to work correctly, the equipartition theorem should be satisfied when there is no electric field. We thus have to choose a dt where this is the case. From 12 we can conclude that we best stay between $dt = 10^{-5}$ and $dt = 10^{-3}$. Although sensitive of timestep, weather the equiparition theorem is satisfied also depends largely on the chosen values of the spring constant, so make sure this value is reasonable.
The smaller deviations, at lower dt, in figure 12 might be due to the dominating noise, as explained in section 5.1.2. The big jump at larger dt is possibly caused by being too large of a timestep to resolve the physics.

7.2. Spring constant

Upon calculating the spring constant, we see in figure 13 that for each calculation, k_{input} lies in the uncertainty of k_{calc}. As expected, the higher the N_t, the smaller the uncertainty. The most accurate obtained value for the spring constant was $k_{\text{calc}} = (5.97 \pm 0.21) \cdot 10^{-5}$ N/m, where the input value was given by $k_{input} = 6 \cdot 10^{-5}$ N/m. This value was obtained with $N_t = 5 \cdot 10^5$ with 100 repetitions. These calculations will not change if we exclude the EDL from the simulation, as the EDL influences the electric field, which is explicitly excluded from these calculations.

7.3. Filtering

A crucial step in calculating the zeta potential is the filtering of the signal. In figure 14 this is shown. At a first glance this filtering seems quite effective. However, the

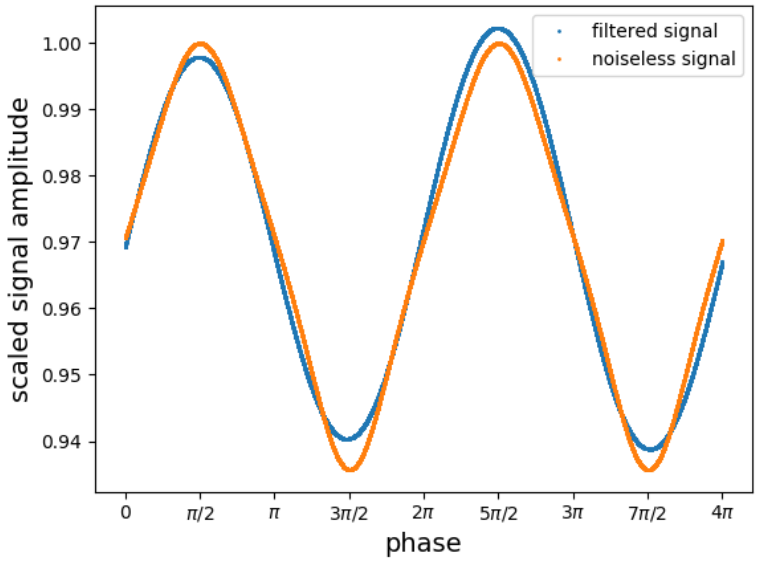

Figure 17.: Comparison of the filtered signal with the original noiseless signal. Both the signals are scaled by the maximum of the noiseless signal.

amplitude of the filtered signal is not quite constant. To compare, I generated the same signal as the one that went into the processing, but left out the noise this comparison can be seen in figure 17. Some improvements could be made on this filtering.

7.4. mobility

When calculating the mobility of the particle, we need to calculate the spring constant first. Since the error in the spring constant propagates to the error in the mobility, I chose to do the calculations with $N_t = 10^5$. This value gave the best balance between minimizing the error and not letting the calculation time get too long. For the experiment however, this balance might be different. The microscope at the nanophotonics group, for example, could only run for small amounts of time before the memory would get full. In this case, the data can be used to estimate the error of your calculation at certain runtimes.
If we look at figure 15, we see a certain shape is repeated. We would expect it to be a straight line, since μ is supposed to be constant. However, filtering even more (for example, only taking the points where the electric field is at least 70% its maximum)

does not resolve this. These shapes thus show that there is some systematic error in each period of the electric field. This error might be due to the error in the filtering. The fluctuations in the height might be explained by the noise that is present, as they are of the same order.

7.4.1. Spring length

In the expression for the electric field, we use the Debye Hückel approximation. In this model the electric field decays exponentially away from the surface. Therefore, we expect that for large l_s, we will be able to less accurately determine the mobility. In figure 16a we can see that this is indeed the case. For a spring length of 25 nm, we achieved the best result, given by $\mu_{\text{calc}} = (3.44 \pm 0.37) \cdot 10^{-8}$.
Beside having greater uncertainties, the values for longer springs are not very far off form the original value. This is an interesting observation, is there a systematic error or are there just a few miss-calculations that causes the error to grow much larger? Figure 16b shows us that the distribution of the value is quite random, so there doesn't seem to be anything unusual.

7.4.2. Applied potential

Lastly, from table 1 we can state that we should keep our applied potential between 0.05 and 0.1 V. Lowering the potential has a similar effect is getting further away from the surface, as it decreases the amplitude of the electric field. Just like the simulation does not allow for a spring length shorter then 18 nm, it doesn't allow for V_0 larger then 0.12 V.

7.5. Effect of the EDL

If we were to ignore the EDL, and only have an electric field due to the applied potential on the parallel plates, we would have a few differences. An important difference is that the filtering of the Brownian motion could be done more accurately as the signal is more even. The electric field will also get a bit stronger when getting closer to the surface. In figure 18 this effect is shown.

7.6. Experiment advice and outlook

To conclude, my advise on carrying out the experiment as described in part I is to use a timestep between $dt = 10^{-5}$ and $dt = 10^{-3}$ seconds. For the simulation, my

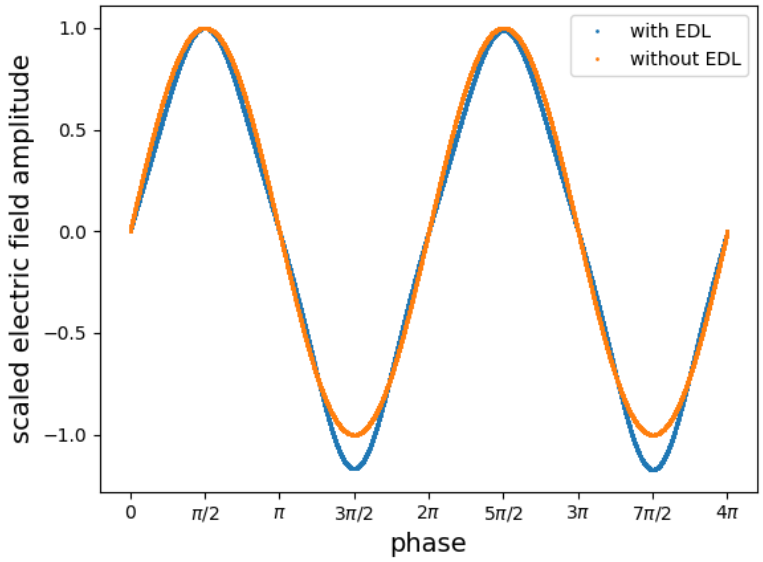

Figure 18.: Comparison of the electric field, at the position of the particle, with (blue) and without (orange) the effects of the EDL. Calculated for $dt = 10^{-5}$ s, $N_t = 10^6$, $l_s = 25$ nm and $V_0 = 0.07$ V. The amplitudes are scaled with their maximum.

advice would be to use $N_t = 10^5$. The optimal size for the nanospring is around 25 nm, with a V_0 of around 0.07 V.

This leaves the floor for improvement of the signal filtering and of course to carry on the original plan of research by using the potentiodynamic optical contrast microscope to look at the sample slides from chapter 3. There is also the possibility of improving the model by simulating the electric double layer in a less approximated way, for example by simulating the EDL in a COMSOL model.

Acknowledgements

I would like to take this moment to thank the people that helped me accomplish the work you have just read. First of all I would like to thank Sanli Faez, who was my main supervisor and he always helped me when I felt stuck. He also found a way to continue my process from home when I wasn't able to finish my work in the lab. And as he always stayed patient, even when he asked me for the 20th time to check the dimensions, for which I am very grateful. I would also like to thank Zhu Zhang, who played a bigger role in the beginning of my project as helped me in operating the microscope.
For finding my way in the labs of the Ornstein building, I would like to show appreciation to Dave van den Heuvel. Dave helped me with the preparations of the samples and with all the highschool chemistry I had long forgotten.
To all the rest of the nanophotonics group I say thank you, for the Tuesday discussions and lectures, for the show and tell coffee meetings and for making me feel part of the group.
The last people I want to mention are my family and friends. Especially my boyfriend Sander, for he was stuck with my cranky mood when my simulation was showing errors again, sorry for that.

Appendices

A. Table of values

The table below shows the values for the parameters used in the simulation unless stated otherwise. The values in the bottom right table are terms used in the python simulation and will not make sense without script.

single values in SI units		
term	value om SI units	numerical value
eps_0	8.85E-12	
kB	1.38E-23	
F	9.65E+04	
NA	6.02E+23	
eta	1.00E-03	
zeta	5.00E-02	
a	1.00E-08	
temp	2.93E+02	
k	6.00E-03	
freq	5.00E+04	
eps_r	80.2	
C0	1.00E+00	
z	1.00E+00	
V0	1.00E-01	
ls	3.00E-08	3.00E+00

Scaling terms	
R0	1.00E-08
T0	1.00E-09

terms calculated from the constants/parameters		
term	value in SI units	numerical value
omg	3.14E+05	3.14E-04
mu	3.55E-08	
drag	1.88E-10	
D	2.15E-11	2.15E-04
kodrag	3.18E+07	3.18E-02
muE	between -0.04 and 0.03	between -0.004 and 0.003
noise	Around +/- 1E-09	around+/- 0.1
kap	103746053.9	1.04E+00
term1	0.186002891	1.86E-02
term2	between -2 and 2	

Bibliography

[1] P. Biesheuvel and J. Dykstra, *Physics of Electrochemical Processes*.

[2] H. Helmholtz, "Ueber einige Gesetze der Vertheilung elektrischer Ströme in körperlichen Leitern mit Anwendung auf die thierisch-elektrischen Versuche," Jan. 1853.

[3] J. Sotres and A. Baró, "Afm imaging and analysis of electrostatic double layer forces on single dna molecules," *Biophysical journal*, vol. 98, no. 9, pp. 1995–2004, 2010.

[4] C. Li and K. J. Kjoller, "Scanning electrochemical potential microscope," Jan. 2 2007. US Patent 7,156,965.

[5] R. F. Hamou, P. Biedermann, A. Erbe, and M. Rohwerder, "Screening effects in probing the electric double layer by scanning electrochemical potential microscopy (secpm)," 2009.

[6] G. Ma, H. Zhu, Z. Wan, Y. Yang, S. Wang, and N. Tao, "Optical imaging of single protein size, charge, mobility, binding and conformational change," *bioRxiv*, 2019.

[7] K. Namink, "Potentiodynamic optical contrast," Master's thesis, Utrecht University, The Netherlands, 12 2019.

[8] B. Svensson, B. Jönsson, and C. E. Woodward, "Monte carlo simulations of an electric double layer," *Journal of Physical Chemistry*, vol. 94, no. 5, pp. 2105–2113, 1990.

[9] J. W. Halley and L. Blum, "Proceedings of the symposium on microscopic models of electrode-electrolyte interfaces," The Electrochemical Society, 1993.

[10] M. R. Philpott and J. N. Glosli, "Screening of charged electrodes in aqueous electrolytes," *Journal of the Electrochemical Society*, vol. 142, no. 2, p. L25, 1995.

[11] E. Spohr, "Molecular simulation of the electrochemical double layer," *Electrochimica Acta*, vol. 44, no. 11, pp. 1697–1705, 1999.

[12] Plasma-Universe, "Debye length," 2017.

[13] J. Lyklema, *Fundamentals of Interface and Colloid Science*. Academic Press, 2005.

[14] M. von Smoluchowski, "Contribution à la théorie de l'endosmose électrique et de quelques phénomènes corrélatifs," *Bull. Akad. Sci. Cracovie.*, vol. 8, pp. 182–200, 1903.

[15] P. Debe and E. Hückel, "Die kataphorese der kugel. phys," *Z*, vol. 25, p. 204, 1924.

[16] D. T. Gillespie, "The mathematics of brownian motion and johnson noise," *American Journal of Physics*, vol. 64, no. 3, pp. 225–240, 1996.

[17] T. Li and M. G. Raizen, "Brownian motion at short time scales," *Annalen der Physik*, vol. 525, no. 4, pp. 281–295, 2013.

[18] C. Gardiner, *Stochastic Methods: A Handbook for the Natural and Social Sciences*. Springer Series in Synergetics, Springer Berlin Heidelberg, 2009.

[19] P. Ullersma, "An exactly solvable model for brownian motion: I. derivation of the langevin equation," *Physica*, vol. 32, no. 1, pp. 27–55, 1966.

[20] "From langevin to fokker-planck equation," may 2014.

[21] X. Durang, C. Kwon, and H. Park, "Overdamped limit and inverse-friction expansion for brownian motion in an inhomogeneous medium," *Phys. Rev. E*, vol. 91, p. 062118, Jun 2015.

[22] P. Weber, D. Ohlendorf, J. Wendoloski, and F. Salemme, "Structural origins of high-affinity biotin binding to streptavidin," *Science*, vol. 243, no. 4887, pp. 85–88, 1989.

[23] S. D. Chandradoss, A. C. Haagsma, Y. K. Lee, J.-H. Hwang, J.-M. Nam, and C. Joo, "Surface passivation for single-molecule protein studies," *JoVE (Journal of Visualized Experiments)*, no. 86, p. e50549, 2014.

[24] S. J. DeCamp, *PEG Coated Slides*. Dogic Lab, 2016.

[25] F. Oesterhelt, M. Rief, and H. Gaub, "Single molecule force spectroscopy by afm indicates helical structure of poly (ethylene-glycol) in water," *New Journal of Physics*, vol. 1, no. 1, p. 6, 1999.

[26] A. Fernandez-Nieves and A. M. Puertas, *Fluids, colloids, and soft materials: an introduction to soft matter physics*. Wiley Online Library, 2016.

[27] R. Pathria, *Statistical Mechanics*. International series of monographs in natural philosophy, v. 45, Elsevier Science & Technology Books, 1972.